

# Generation of bright, tunable, polarized $\gamma$ -ray sources by scattering laser pulses from APS electron beams

Yuelin Li

*The Advanced Photon Source, Argonne National Laboratory, Argonne, IL 60439.*

Email: ylli@aps.anl.gov

## Abstract

We calculate the performance of possible APS (Advanced Photon Source)  $\gamma$ -ray sources for applications in nuclear physics research. For the APS storage ring, it is possible to generate  $\gamma$ -ray photon fluxes of  $10^8$  photons/s at 1, 1.7, and 2.8 GeV while for the injection booster, a  $\gamma$ -ray photon flux up to  $10^8$  photons/s at energy ranging from 5 MeV to 1 GeV is possible. Those can be achieved using off-the-shelf commercial Ti: Sa laser systems.

## I. Introduction

The use of Compton scattering of laser beams from high-energy electron beams to generate high-energy photons was proposed in 1963 [1,2] and has since been implemented using commercial lasers on electron storage rings to produce highly polarized photons in the energy range useful for nuclear physics [3-7].

Most of the existing facilities are built at synchrotron light sources such as GRAAL at ESRF [4], LEPS at SPring-8 [5], and LEGS at NSLS [6], where the stored beam is used as the electron source. As such, the depletion of the stored electron beam is the main obstacle for generating higher photon fluxes. As a result, the photon flux obtained is normally limited at a level of about  $10^6$ /s [3]. Only the future HIGS (high intensity gamma-ray source), based on the intracavity scattering with a free-electron laser at Duke University, boasts photon flux higher than  $10^7$ /s while the highest photon energy is limited at 200 MeV [7].

In this note, we propose to use the stored electron beams in the APS storage ring or the injection booster for generating  $\gamma$ -rays where the effect of the electron depletion can be mitigated or is nonexistent. For the storage ring, since it is operating in the “top-up” mode, i.e., the stored electron beam is replenished by frequent injections, the depletion of the beam can be easily compensated by either higher injection charge or more frequent injections. The relatively infrequent injection, on the other hand, makes it possible to store beams in the injection booster solely for generating Compton  $\gamma$ -rays between injections.

## II. APS Compton scattering source performance

### 2.1 APS storage ring and the injection booster

The APS comprises four successive accelerators: the injection linac, the particle accumulation ring (PAR), the injection booster, and the APS storage ring. In this note, we consider the booster and the storage ring as the potential electron beam sources. The beam parameters of the two rings are listed in Table 1.

The role of the injection booster is to ramp up the energy of the electron bunches from the injection linac or PAR from 400 MeV to 7 GeV, and inject them into the APS storage ring, where the beam is stored to generate synchrotron radiation for users. The booster is capable of storing electron beams with energy up to 4 GeV and a duty cycle of 2 Hz. The beam rate, determined by the circumference of the ring, is 815 kHz. The APS storage ring (SR), with a circumference three times that of the booster, stores electrons at up to 7 GeV of energy, normally with 23 bunches, each with 15 nC of charge.

Unique to the operation of the APS is the “top-up” operation mode, in which frequent injections are made into the storage ring to compensate for the lost electrons. Currently, injection is at 2-3 nC every two mins, indicating a beam decay rate of  $10^8$   $e^-$  per second. Note that, in the current transverse injection scheme, a beam perturbation is induced at every injection by displacement of the beam during the injection. The 2-min injection interval is

**Table 1. APS Booster and Storage Ring (SR) Beam Parameters**

	Booster	APS SR ID	APS SR BM
Revolution frequency (kHz)	815	272	
Injection frequency $F_i$ (Hz)	2	0.008	
Nominal energy (GeV)	7	7	
Stored beam energy (GeV)	0.45-4	7	
Energy gain per turn (keV)	32.0	-	
Energy spread, rms @ 7-GeV	0.1%	0.1%	
Emittance $\epsilon_0$ @ 7 GeV (m-rad)	$130 \times 10^{-7}{}^a$	$2.5 \times 10^{-9}$	
Coupling factor $k$	0.1	0.01-0.03	
Electrons per bunch	$6.25 \times 10^{10}$ (10 nC) $^b$	$10^{11}$ (15 nC)	
Number of bunches	1	23 $^c$	
Bunch repetition rate (kHz)	815	6528	
Bunch length, rms, @ 7 GeV (ps)	77	45	
Beta functions $\beta_{x,y}$ (m)	16, 2.7	19.5, 2.9	2.12, 26.1
Beam size $\sigma_x, \sigma_y$ ( $\mu\text{m}$ )	786, 102	274, 8.5	91.8, 25.5
Beam divergence $\sigma_x, \sigma_y$ ( $\mu\text{rad}$ )		11.3, 2.9	56.3, 1.1

- a.* Recent enhancement to the focus of the magnets has improved this down to 93 nm rad [8].
- b.* This is determined by the radiation safety envelope. The highest ever achieved is 4-5 nC.
- c.* The typical bunch pattern is 23 bunches spaced evenly at 1/24 of the ring's circumference with the 24<sup>th</sup> bunch missing.

determined by the balance between maximum tolerable beam perturbation by the users and a beam current stability of about 1%.

A perturbation-minimized longitudinal injection scheme has been demonstrated. This new scheme enables more frequent injections but will need a different lattice for operation [9]. If implemented, injection at the booster duty cycle of up to 2 Hz is possible.

## 2.2 Possible performance of the proposed $\gamma$ -ray sources

The maximum photon energy and the corresponding scattering cross section as a function of the electron beam energy accessible at the APS are plotted in Fig. 1 (a) and (b) for laser photon energies of 1.55, 3.10, and 6.20 eV. The laser is a Ti:Sa laser system working at the fundamental, second, and fourth harmonics (see Section 2. 4 for laser requirement). Also plotted in Fig. 1 (c) is the maximum transferable linear polarization. The calculations are based on the formula given in Appendix A. With the booster, photon energies from a few MeV to 1 GeV are possible, while with the SR the highest photon energy accessible is 2.8 GeV at 7 GeV electron beam energy.

### 2.2 a. The booster case

Using the formula developed in Appendix B, the calculated photon fluxes and the beam lifetime as a function of the photon energy are shown in Figs. 2 and 3 for the booster and the APS storage ring, respectively. Here the highest achieved charge of 5 nC in one bunch is used while the normal operation charge is 2-3 nC currently. The intrabeam scattering effect (see Appendix B, section 2) is included. An off-the-shelf laser system with 2.5 W of average power at the fundamental wavelength of 800 nm (Coherent RegA9000, see Table C1) is used for its closely matched repetition rate. Conversion efficiencies of 50% and 15% to the second harmonic (SH) and the fourth harmonic (FH), respectively, are used in the calculation. The photon fluxes depicted in Fig. 2 represent the immediately achievable performance of the system.

Clearly, a wide tuning range is easily achievable with the booster. Using the laser fundamental, the energy ranges from 6 MeV to 100 MeV, while with the fourth harmonic of the same laser, the highest photon energy is 1 GeV. The photon flux is about  $10^8$ /s at 100 MeV, while at 1 GeV it drops to  $2 \times 10^6$ /s.

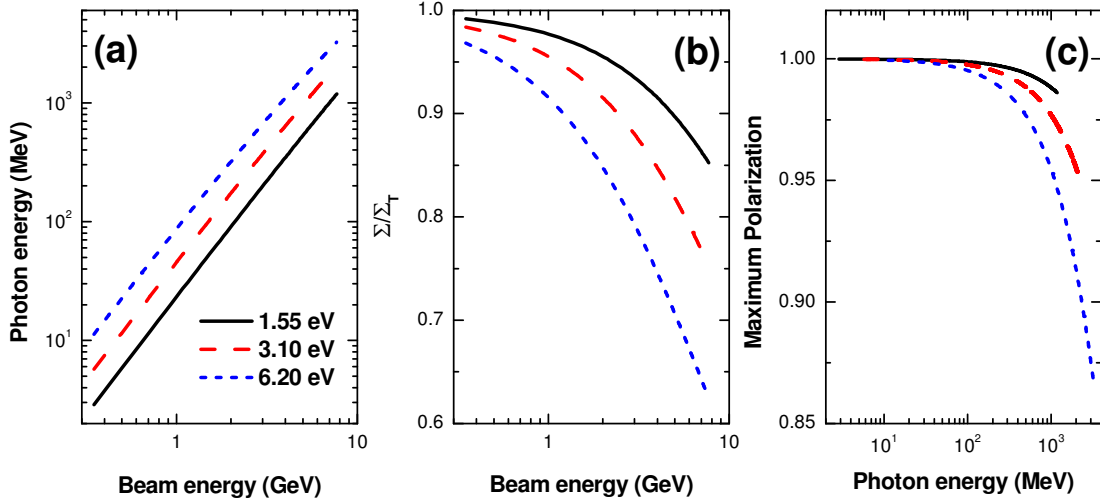


**Fig. 1** (a) Gamma ray photon energy and (b) total scattering cross section  $\Sigma$  normalized to the Thomson scattering cross section of  $\Sigma_T = 8\pi r_e^2/3 = 0.665 \times 10^{-24} \text{ cm}^2$  as a function of the beam energy for laser photon energies of 1.55, 3.1, and 6.2 eV; (c) the maximum transferable linear polarization as a function of the photon energy.

To push for the 10-nC charge as limited by the safety envelope, improvement of the rf cavity tuner is needed to compensate the beam loading. Also, the beam quality may be improved by replacing the existing magnets. At the time of this writing, the emittance has been improved from 130 nm rad to 90 nm rad by implementing a new lattice, a 30% improvement [8]. Furthermore, with a modest development effort, it is possible to develop a laser system with much higher power. In fact, a 30-W, 75-MHz laser is under construction at the Jefferson National Accelerator Facility (JLab) [10].

Taking into account all of these possible improvements, especially the laser, a tenfold improvement in photon flux across the energy spectrum is expected in the near future, which gives photon fluxes higher than  $10^9/\text{s}$  at

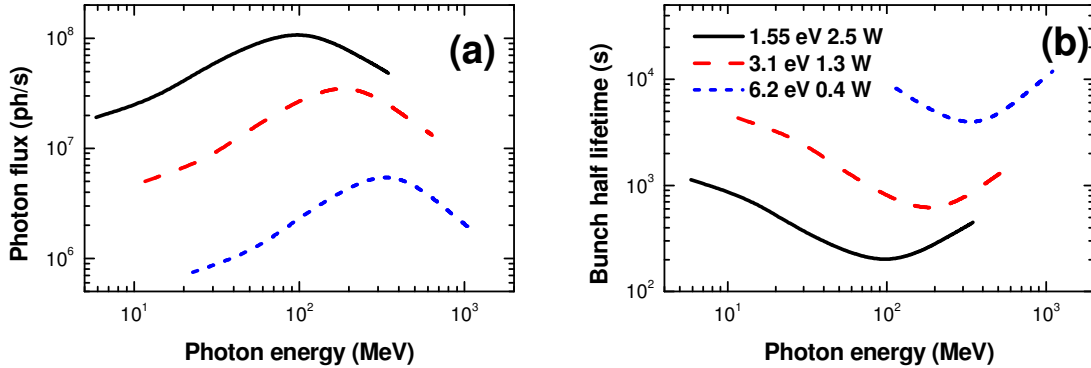


**Fig. 2** (a) Photon flux and (b) beam half lifetime as functions of photon energy for the APS booster. Here a laser with 300-ps pulse duration, 2.5-W average power at 800-nm fundamental wavelength is used, and conversion efficiencies of 50% and 15% to the second harmonic (SH) and the fourth harmonic (FH) are assumed. The laser is assumed to have a repetition rate matching that of the booster beam rate of 815 kHz. A 5-nC charge is used in the calculation. Note that the bunch lifetime is for a single bunch.

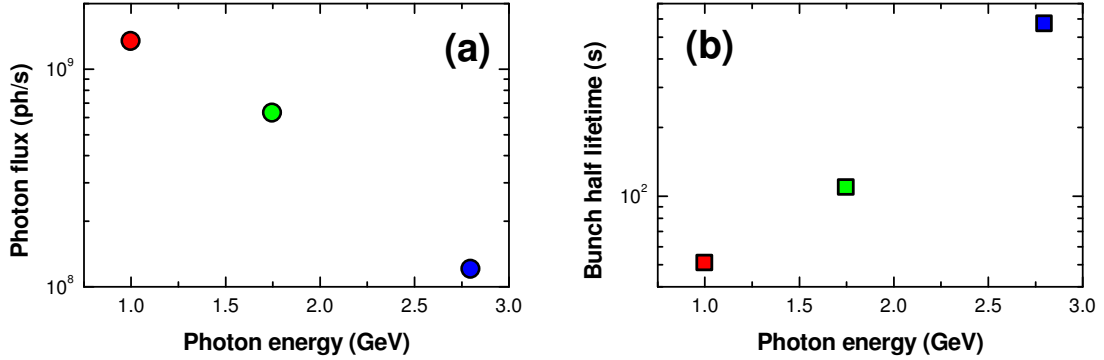


**Fig. 3** (a) Photon flux and (b) bunch lifetime for the APS SR with a 3.5-W laser working at the fundamental, SH, and FH of 800 nm, 400 nm, and 200 nm. Conversion efficiencies to the SH and FH of 50% and 15% are used. The fundamental, SH, and FH generate  $\gamma$ -ray photon energies of 1, 1.7, and 2.8 GeV, respectively. The bunch lifetime is calculated for a single bunch when the laser is at 272 kHz, matching the beam revolution rate. If the laser is interacting with more than one bunch at higher repetition rates but the same average power, the lifetime should be multiplied by the bunch number. In all cases the depletion rate or photon flux is higher than the current injection rate of  $10^8$  e<sup>-</sup>/s.

100 MeV and  $2 \times 10^7$ /s at 1 GeV. Ultimately, the photon flux is limited by the duty cycle of the booster (2 Hz) and the maximum safety envelope.

### 2.2.b The APS storage ring case

In comparison, the APS SR case seems to be more attractive, mainly due to the much higher beam quality and higher charge per bunch, and mostly to the ‘top-up’ operation mode.

There are two possible locations for the Compton scattering setup as listed in Table 1: the insertion device (ID) position and the bending magnet (BM) position. We will only consider the BM location as the ID locations are all occupied.

The calculations plotted in Fig. 3 use the current beam parameters in Table 1. The laser is the 3.5-W Spectra Physics Tsunami laser at 800 nm. Again, conversion efficiencies of 50% and 15% to the SH and the FH are assumed. The repetition rate of the laser (80 MHz) can be slowed using an external cavity fitted with an acoustic optical modulator as a cavity dumper [11] to match up to 24 times the revolution rate of the beam for the 23-bunch pattern at 6.52 MHz, or in case of more electron bunches, up to the bunch repetition rate. The advantage of such an optical cavity is that it can be designed to accommodate different bunch patterns in the storage ring to maximize the scattering rate.

Obviously, in Fig. 3, the photon fluxes of  $10^9$ ,  $6 \times 10^8$ , and  $10^8$ /s at 1, 1.7, and 2.8 GeV, respectively, exceed or equal the electron replenishing rate of  $10^8$  e<sup>-</sup>/s in the current injection mode, i.e., 2-3 nC per injection every two minutes. With the maximum achieved charge per injection of 4-5 nC at the current interval of two min, the photon fluxes at 1 GeV and 1.7 GeV are limited by the injection charge at  $1-2 \times 10^8$ /s, while at 2.8 GeV the photon flux is limited at  $10^8$ /s. These represent the immediately achievable performances, and are generally one to two orders of magnitude better than the existing facilities at the same photon energy [3].

Moreover, although a higher charge per injection is not immediately achievable due to the limitation of the booster, more frequent injections seem to be a relatively easy and low-risk operation mode to implement using the above-mentioned longitudinal injection scheme [9]. This will significantly raise the photon flux at 1 GeV and 1.7 GeV, up to  $10^9$  and  $6 \times 10^8$  photons/s, respectively, with the same 3.5-W laser. With a laser 10 times more powerful, up to  $3 \times 10^9$ ,  $2 \times 10^9$ , and  $3 \times 10^8$  photons/s can be obtained at 1, 1.7, and 2.8 GeV. The ultimate limitation is the radiation safety envelope of 10 nC per injection and the duty cycle of 2 Hz of the booster, which translates to  $10^{11}$  photons/s.

### 2.3 Divergence, spectrum, and polarization

The divergence of the photon beam is determined by the energy of the beam of  $1/\gamma$ . From Eq. (A1) in Appendix A, the spectrum with a collimating angle  $\Delta\theta$  is a convolution of beam (laser and electron) divergence and energy spread. In our cases, due to the high photon energy, electron tagging and photon collimation are needed for the desired energy resolution [3].

The polarization is proportional to that of the laser in both the circular and linear polarization case. For the linear polarization case, the maximum transferable polarization will be reduced due to the spin flip in the electron bunches [3], as given in Eq. (A4) in Appendix A and shown in Fig. 1 (c).

### 2.4 The laser

In practice, electron tagging prefers higher duty cycle to higher peak brightness. In addition, the laser has to be synchronized to the electron beam with a jitter of several picoseconds for stable operation. This requires the laser system to be an oscillator-amplifier configuration or just an oscillator, which is temporally locked to the rf of the accelerators. A few of the off-the-shelf laser systems are listed in Appendix C for reference. The challenge is to tailor the laser to the required repetition rate while maintaining the power. For example, an external Fabry-Perot cavity with an acoustic optical modulator cavity dumper can be used to adjust the repetition rate while maintaining the optical power [11].

In the above calculation, we used two commercial Ti:Sa laser systems with a few watts of output as examples. Higher laser power up to a few tens of watts can be obtained. For example, as mentioned earlier, a Ti:Sa laser of 30 W average power at 75 MHz is under construction at JLab [10], and the development effort is described as modest. Another alternative, though more difficult to implement without modifying the electron beam trajectory, is to use an intracavity scattering scheme in an oscillator or with an external Fabry-Perot cavity. The intracavity optical power can be orders of magnitude higher than the direct output power from the laser.

We use a Rayleigh length of 300 ps for the fundamental in our calculation. Using Eq. (B6) in Appendix B, the optimum laser spot size is  $\sigma_0=76\text{ }\mu\text{m}$ , 38, and 19  $\mu\text{m}$  for the fundamental, second, and fourth harmonics for a common set of focusing optics, respectively. We further assume 50% and 15% conversion efficiencies for the second and fourth harmonics.

### 2.5 Operation

Obviously, the SR and the booster have opposite requirements in the operation mode and cannot be fulfilled simultaneously. While the SR  $\gamma$ -ray source can significantly benefit from a more frequent injection, the source proposed for the booster prefers less frequent injection for more dedicated beam time for generating the  $\gamma$ -ray beam. Even in the current operation mode, 20 seconds out of the 2-min interval is needed to prepare the booster for injection.

For the SR scheme, the depletion of the electrons has to be considered as an integrated part of the operation to correctly set up the operation mode so that if the laser is down for any reason, the top-up injection can be automatically adjusted to accommodate the change.

In addition, to more efficiently use the injected electrons, dedicated bunches can be assigned for scattering. These bunches are refreshed more often than others to maintain the  $\gamma$ -ray photon flux. They can be allocated to any evenly distributed pattern up to all the stored bunches. In this regard, a buffer optical cavity with the configuration described in ref. [11] will be necessary for adjusting the laser repetition rate to achieve high average fluxes while minimizing the peak fluxes.

**Table 2. Comparison of the Performance of the Proposed APS  $\gamma$ -Ray Source and HIGS**

	APS SR	APS booster	ESRF GRAAL [3]	SPring-8 LEPS [3]	HIGS future [3]
Beam energy (GeV)	7	0.4-4	6	8	0.2-1.3
$\gamma$ -ray energy (GeV)	1, 1.7, 2.8	0.005-1.0	0.55-1.50	1.5-2.4	0.002-0.220
Flux (photons/s)			$3 \times 10^6$	$5 \times 10^6$	$10^6$ - $10^{10}$
Immediate	$1$ - $2 \times 10^8$	$2 \times 10^6$ - $10^8$			
Foreseeable upgrade	$3 \times 10^9$ - $3 \times 10^8$	$2 \times 10^7$ - $10^9$			
Machine limit	$10^{11}$	$10^{11}$			

## 2.6 Comparison with other $\gamma$ -ray sources

Table 2 summarizes the immediate and future performances of the proposed APS storage ring/booster  $\gamma$ -ray sources and compares those with the performance of GRAAL [4], LEPS [5], and future HIGS [7]. It is believed that HIGS will be the brightest  $\gamma$ -ray source when commissioned.

In Table 2, there are three flux entries for the APS sources. The entry ‘immediate’ represents those that can be available now with existing commercial laser systems and no change in the hardware and operation mode for the accelerator systems. The entry ‘foreseeable’ represents those with achievable laser performances after modest development effort and changes in the operation modes of the accelerator systems. The entry ‘machine limit’ represents those that can be achieved only after full accelerator system hardware upgrades and operation scheme optimization, together with state-of-the-art laser system upgrades.

To summarize from Table 2, the major advantages of the two proposed APS  $\gamma$ -ray sources are:

- 1) High photon fluxes of up to  $10^8$ /s, comparable with future HIGS photon fluxes of  $10^6$ - $10^{10}$ /s and about two orders of magnitude higher than those at GRAAL and LEPS;
- 2) An ultrabroad tuning range from 5 MeV to 1 GeV for the booster source and high photon energy of 2.8 GeV for the storage ring in comparison with the 2- to 200-MeV range at HIGS, and the 1.5 GeV and 2.4 GeV available at GRAAL and LEPS, respectively;
- 3) With developing laser technologies and upgrades to the operation mode of the APS machines, photon fluxes of  $10^{11}$ /s are possible, limited only by the machines’ safety envelopes.

## III. Summary

Due to the particular operation mode of the APS storage ring and booster, our calculations show that with currently available laser technology and the existing operation lattice, it is possible to build  $\gamma$ -ray radiation sources with high photon fluxes at photon energies from a few MeV to 2.8 GeV. If built, either one will become an extremely useful  $\gamma$ -ray source for nuclear physics applications.

**Acknowledgement** Many people have contributed to this feasibility study, including S. V. Milton, L. Emery, N. Sereno, V. Sajaev, Y. Chae, J. Lewellen, K. Harkay, and Z Huang (now at SLAC) of the Advanced Photon Source; B. Berman and J. Feldman at George Washington University. G. Neil at JLab, and V. Litvinenko at HIGS also contributed very useful comments and criticisms. This work is supported by the U. S. Department of Energy, Office of Basic Energy Sciences, under Contract No. W-31-109-ENG-38.

## References

1. R. H. Milburn, Phys. Rev. Lett. **10**, 75 (1963).
2. F. R. Arutyunyan, V. A. Tumanian, Phys. Lett. **4** (1963).
3. A. D’Angelo et al., NIM **A455**, 1 (2000), and references therein.
4. J.P. Bocquet et al., Nucl. Phys. A **622**, 124c (1997).
5. T. Nakano et al., Nucl. Phys. A **684**, 71c (2001).
6. A. M. Sandorfi et al., IEEE Trans. NS-30, B **3083** (1983);

7. T. S. Carman, NIM A **378**, 1 (1996); HIGS collaboration, "A Proposal for the Support of a Free -Electron Laser Generated High-Intensity  $\gamma$ -Ray Source for Nuclear Physics," available on-line at <http://www.tunl.duke.edu/Local/proposal/higs/>.
8. This will result in an approximately 30% improvement of the photon flux over those in this note for the booster, especially for high-energy operations where the intrabeam scattering effect is negligible.
9. Y. Chae, private communication.
10. G. Neil, private communication.
11. R. J. Jones and J. Ye, Opt. Lett. **27**, 1848 (2002).
12. V. B. Berestetskii, E. M. Lifshitz, and L. P. Pitaevskii, Quantum Electrodynamics, 2<sup>nd</sup> edition, Chapter X (Pergamon, New York, 1994).

## Appendix A: Basics of Compton scattering

### A.1 $\gamma$ -ray photon energy and scattering cross section

For head-on scattering ( $\phi=\pi$ ), the energy of the scattered photons scales as

$$E_s = \frac{4\gamma^2 E_L}{1 + \frac{4\gamma E_L}{mc^2} + (\theta\gamma)^2}. \quad (\text{A1})$$

Here  $\gamma$  is the relativistic factor of the electron beam,  $E_L$  is the laser photon energy,  $m$  is the electron mass, and  $\theta$  is the scattering angle of the photon from the electron propagation direction. The total scattering cross section is [12]

$$\Sigma = \frac{2\pi r_e^2}{x} \left[ \left( 1 - \frac{4}{x} - \frac{8}{x^2} \right) \ln(1+x) + \frac{1}{2} + \frac{8}{x} - \frac{1}{2(1+x^2)} \right]. \quad (\text{A2})$$

Here  $r_e$  is the classical electron radius, and

$$x = \frac{2\gamma E_L (1 - \beta \cos \phi)}{mc^2} = \frac{4\gamma E_L}{mc^2}. \quad (\text{A3})$$

### A.2 Polarization

The degree of polarization of the scattered photons is proportional to that of the laser beam for both linear and circular polarization, and the polarization is highest at the Compton edge (highest photon energy) where the spin-flip amplitude for highly relativistic electrons vanishes. In the linear polarization case, there is a drop of the maximum transferable polarization at high photon energy [3]:

$$P_{\gamma \max} = P_{\text{Laser}} \frac{2}{2 + \frac{(1-a)^2}{a}}. \quad (\text{A4})$$

Here  $a=1/(1+x)$ , with  $x$  defined in Eq. (A3).

## Appendix B: Photon flux and electron beam lifetime

### B.1 Calculation of photon flux

Consider an electron bunch with the following distribution

$$f_e = \frac{N_e}{(2\pi)^{3/2} \sigma_x \sigma_y \sigma_z} \exp \left( -\frac{x^2}{2\sigma_x^2} - \frac{y^2}{2\sigma_y^2} - \frac{(z-ct)^2}{2\sigma_z^2} \right), \quad (\text{B1})$$

with transverse rms beam size of

$$\begin{aligned} \sigma_x &= \sqrt{\frac{\varepsilon_0 \beta_x}{1+k}} \frac{\gamma}{\gamma_0}, \\ \sigma_y &= \sqrt{\frac{k \varepsilon_0 \beta_y}{1+k}} \frac{\gamma}{\gamma_0}, \end{aligned} \quad (\text{B2})$$

and an rms longitudinal bunch size of  $\sigma_z$ . Here  $N_e$  is the total number of electrons,  $\varepsilon_0$  is the emittance at beam energy  $\gamma_0$ ,  $k$  is the coupling factor, and  $\beta_{x,y}$  are the beta functions of the electron beam, the equivalent of the Rayleigh range in optics.

Similarly, we assume the laser has the following distribution at the focus:



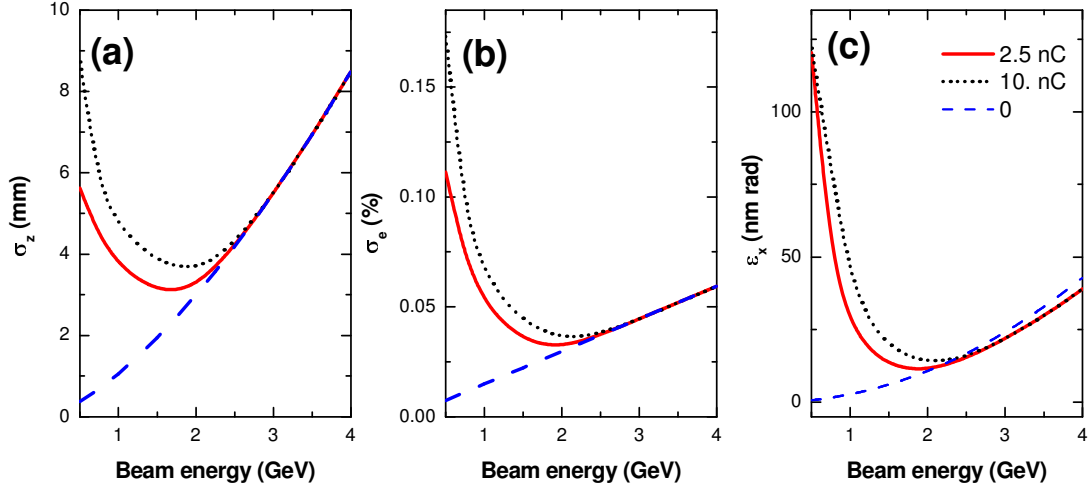


**Fig. B1** The effect of intrabeam scattering on the electron (a) bunch length, (b) energy spread, and (c) emittance, for ideal (0-nC), 2.5-nC, and 10-nC charges for the APS booster.

$$f_p = \frac{N_p}{(2\pi)^{3/2} \sigma_0^2 \sigma_t} \exp\left(-\frac{x^2 + y^2}{2\sigma_0^2} - \frac{(z/c + t)^2}{2\sigma_t^2}\right), \quad (\text{B3})$$

with an rms pulse width of  $\sigma_t$  and beam waist  $w_0=2\sigma_0$ . Here  $N_p$  is the total number of photons per pulse. The total number of  $\gamma$ -ray photons per shot is calculated as

$$N_\gamma = \Sigma \int \int \int \int f_e f_p dx dy dz dt. \quad (\text{B4})$$

The integration yields

$$N_\gamma = \Sigma \frac{N_e N_p}{2\pi \sqrt{\sigma_0^2 + \sigma_x^2} \sqrt{\sigma_0^2 + \sigma_y^2}}. \quad (\text{B5})$$

Obviously, with given  $\sigma_x$  and  $\sigma_y$ ,  $\sigma_0$  is the key factor that determines the flux: the smaller the  $\sigma_0$ , the higher the flux. On the other hand, Eqs. (B4-B5) require the laser Rayleigh length,  $Z_R=\pi w_0^2/\lambda$ , to be equal to or larger than the larger of the FWHM of the laser pulse,  $c\tau_L$ , and the electron bunch length,  $2\sqrt{2\ln 2}\sigma_z$  (the beta functions of the electron beams are normally very large, hence are not considered a limitation). Assuming that the laser pulse duration is the larger, the optimum laser spot size is approximately

$$\sigma_0 \approx \sqrt{\frac{c\tau_L\lambda}{4\pi}}. \quad (\text{B6})$$

When using lasers at different wavelengths, the beam waist scales with the wavelength if the focusing optics is maintained at the same  $f$ -number.

## B.2 Electron bunch lifetime

Rewriting Eq. (B5) as a production rate per shot  $r=N_\gamma/N_e$ , for a repetition rate of  $f$  and  $fr \ll 1$ , the total flux  $F$  and the beam half lifetime  $T$  are

**Table C1. Performance of the Off-the-Shelf Ti:Sa Lasers**

Make and model	Energy per pulse <sup>a</sup>	Rep rate	Average power
Coherent RegA9000	5 $\mu$ J compressed 10 $\mu$ J uncompressed	250 kHz	2.5 W
Quantronix	>5 mJ compressed 10 mJ uncompressed	1 kHz	10 W
Spectra Physics Tsunami	40 nJ	80 MHz	3.5 W
Coherent Mira	20 nJ	80 MHz	1.4 W

a. In deriving the uncompressed pulse energy, the compressor efficiency is assumed to be 50%.

$$F = rN_e \sum_{j=0}^{f-1} (1-r)^j = N_e [1 - (1-r)^f] \approx rfN_e, \quad (B7)$$

$$T = -\frac{1}{f} \frac{\ln 2}{\ln(1-r)} \approx \frac{\ln 2}{fr}.$$

### B.3 Effect of the intrabeam scattering

In a storage ring, the beam quality is determined by quantum excitation and radiation damping of the electrons. At low beam energies, the intrabeam scattering will cause the bunch length, energy spread, and emittance to grow. These effects are shown in Fig. B1 (a-c), respectively, for the APS booster at bunch charges of 10, 2.5, and 0 nC.

## Appendix C: Off-the-shelf laser systems

The performance of several off-the-shelf laser systems is listed in Table C1 for reference. Note that these commercial lasers only represent the standard performance one can achieve with such systems. With modest development effort, laser systems with performances far exceeding these can be built [11].